Author's Accepted Manuscript

Engineering meniscus structure and function via multi-layered mesenchymal stem cell-seeded nanofibrous Scaffolds

Matthew B. Fisher, Elizabeth A. Henning, Nicole Söegaard, Marc Bostrom, John L. Esterhai, Robert L. Mauck

Cite this article as: Matthew B. Fisher, Elizabeth A. Henning, Nicole Söegaard, Marc Bostrom, John L. Esterhai, Robert L. Mauck, Engineering meniscus structure and function via multi-layered mesenchymal stem cell-seeded nanofibrous Scaffolds, *Journal of Biomechanics,* http://dx.doi.org/10.1016/j.jbiomech.2015.02.036

This is a PDF file of an unedited manuscript that has been accepted for publication. As a service to our customers we are providing this early version of the manuscript. The manuscript will undergo copyediting, typesetting, and review of the resulting galley proof before it is published in its final citable form. Please note that during the production process errors may be discovered which could affect the content, and all legal disclaimers that apply to the journal pertain.

Engineering Meniscus Structure and Function via Multi-layered Mesenchymal Stem Cell-seeded Nanofibrous Scaffolds

Matthew B. Fisher, PhD[a,b]; Elizabeth A. Henning, BS[a,b]; Nicole Söegaard, BS[a]; Marc Bostrom, MS[a]; John L. Esterhai, MD[a,b]; Robert L. Mauck, PhD[a,b,c*]

[a]*McKay Orthopaedic Research Laboratory, Department of Orthopaedic Surgery, Perelman School of Medicine, University of Pennsylvania, Philadelphia, PA 19104, USA*

[b]*Translational Musculoskeletal Research Center, Philadelphia VA Medical Center, Philadelphia, PA 19104, USA*

[c]*Department of Bioengineering, University of Pennsylvania, Philadelphia, PA 19104, USA*

Word Count (Introduction to Discussion): 4629

*Corresponding Author:
Robert L. Mauck, PhD
Associate Professor
Department of Orthopaedic Surgery
Perelman School of Medicine, University of Pennsylvania
424 Stemmler Hall
36th Street and Hamilton Walk
Philadelphia, PA 19104
Phone: 215-898-3294
Fax: 215-573-2133
Email: lemauck@mail.med.upenn.edu

Abstract

Despite advances in tissue engineering for the knee meniscus, it remains a challenge to match the complex macroscopic and microscopic structural features of native tissue, including the circumferentially and radially aligned collagen bundles essential for mechanical function. To mimic this structural hierarchy, this study developed multi-lamellar mesenchymal stem cell (MSC)-seeded nanofibrous constructs. Bovine MSCs were seeded onto nanofibrous scaffolds comprised of poly(ε-caprolactone) with fibers aligned in a single direction (0° or 90° to the scaffold long axis) or circumferentially aligned (C). Multi-layer groups (0°/0°/0°, 90°/90°/90°, 0°/90°/0°, 90°/0°/90°, and C/C/C) were created and cultured for a total of 6 weeks under conditions favoring fibrocartilaginous tissue formation. Tensile testing showed that 0° and C single layer constructs had stiffness values several fold higher than 90° constructs. For multi-layer groups, the stiffness of 0°/0°/0° constructs was higher than all other groups, while 90°/90°/90° constructs had the lowest values. Data for collagen content showed a general positive interactive effect for multi-layers relative to single layer constructs, while a positive interaction for stiffness was found only for the C/C/C group. Collagen content and cell infiltration occurred independent of scaffold alignment, and newly formed collagenous matrix followed the scaffold fiber direction. Structural hierarchies within multi-lamellar constructs dictated biomechanical properties, and only the C/C/C constructs with non-orthogonal alignment within layers featured positive mechanical reinforcement as a consequence of the layered construction. These multi-layer constructs may serve as functional substitutes for the meniscus as well as test beds to understand the complex mechanical principles that enable meniscus function.

1. Introduction

The menisci are crescent-shaped fibrocartilaginous tissues that function to transmit and distribute complex loads between the femur and tibia at the knee joint. Meniscus function is enabled by the hierarchical organization of the extracellular matrix (ECM), including bundles of highly aligned collagen fibers that circumnavigate the tissue between the insertion sites on the tibial plateau. These fiber bundles bear tensile hoop stresses when the wedge-shaped meniscus is compressed axially, thereby increasing the contact area over which loads are transmitted and decreasing stress concentrations on the opposing articular cartilage (Ahmed, et al., 1983, Kurosawa, et al., 1980, Maher, et al., 2010, Zielinska, et al., 2006). In addition, the meniscus contains radial bundles that are orthogonal to and interdigitate with circumferentially aligned bundles (Andrews, et al., 2014, Petersen, et al., 1998). These tie fibers provide additional mechanical reinforcement and are thought to prevent separation of circumferentially aligned bundles. Together, this organized and hierarchical collagenous ECM endows the tissue with highly anisotropic mechanical properties in tension, which are highest in the circumferential direction (Bursac, et al., 2009, Fithian, et al., 1990, Makris, et al., 2011, Proctor, et al., 1989, Skaggs, et al., 1994).

Injuries to the meniscus are common, though the complex nature of these injuries often renders suture-based repairs ineffective or impossible (Garrett, et al., 2006, Greis, et al., 2002). As a result, partial removal of the meniscus represents the most commonly performed orthopaedic surgery in the U.S. (Garrett, et al., 2006, Lubowitz, et al., 2011), despite the fact that removal increases the likelihood of osteoarthritis (Bedi, et al., 2010, Lubowitz, et al., 2011, Petty, et al., 2011)(3), and recent evidence showing little if any

improvement in patient outcomes compared to no treatment for degenerative meniscus injuries (Sihvonen, et al., 2013). Though less common, severe injuries may be treated via replacement of the entire meniscus with allograft tissue. However, issues with these grafts include donor availability, size matching, disease transmission, incomplete cellular incorporation post-surgery, and poor integration to the surrounding tissues (Greis, et al., 2002). In order to overcome these limitations, a number of tissue engineered (TE) constructs and scaffolds have been developed to replace portions of the damaged meniscus (Aufderheide, et al., 2007, Ballyns, et al., 2011, Cook, et al., 2006, Heijkants, et al., 2004, Kelly, et al., 2007, Mandal, et al., 2012, Stone, et al., 1992, Veth, et al., 1986). An increasing number of these engineered materials have focused on matching macro- and micro- structural features of native tissue that enable its complex load bearing function. This has been achieved by scaffold processing techniques (to 'engineer in' scaffold organization) or through stimulation of cells within constructs to generate aligned and hierarchically organized matrix (via the provision of topographical and mechanical cues) (Aufderheide, et al., 2007, Balint, et al., 2012, Kelly, et al., 2007, Puetzer, et al., 2013).

While promising, these approaches have not yet culminated in cellularized constructs possessing the macroscopic and microscopic multi-scale structure and function of the native meniscus. For example, aligned nanofibrous scaffolds produced via electrospinning can recapitulate the mechanical anisotropy of the meniscus over small length scales (millimeters) (5,6), and seeding with human meniscus cells increased tensile properties with time in culture by directing organized tissue formation (Baker, et al., 2007). Further, production of these scaffolds can be modified so as to replicate the

4

circumferential macroscopic orientation of fibers within a single plane over longer length scales (centimeters) (7). Despite these advances, it remains a challenge to generate scaffolds matching the anatomic size and shape of the meniscus while allowing for complete cellular infiltration upon implantation. Moreover, anatomic directionality and hierarchical organization into orthogonal fiber structures (circumferential and radial tie fibers) has not yet been investigated.

To address these limitations, the current study developed methods to assemble individual cell-seeded layers to form multi-layer constructs that replicate the micro- and macro-scopic structure and function of the meniscus. These methods were originally developed for the annulus fibrosus (AF) of the disc (Driscoll, et al., 2011, Nerurkar, et al., 2009). In those studies, newly formed ECM within and between layers that were oriented in an angle ply configuration (+/-30° with respect to the long axis, similar to the native AF) produced a reinforcing effect via ECM mediated resistance to shearing between the layers. Here, we extend this concept to the evaluation of a three layer scaffold seeded with mesenchymal stem cells (MSCs) where layers were assembled in an orthogonal pattern to mimic the circumferential and radial tie fibers of the native meniscus. Additionally, unlike the AF which features layers with fibers that are preferentially aligned in a single direction, the meniscus consists largely of circumferential fibers that change in their spatial orientation, which we also engineered into our multi-layer scaffolds using a recently developed technology (Fisher, et al., 2013). We hypothesized that the different multi-layer construction algorithms would yield different mechanical outcomes, with increasing properties in constructs containing a greater fraction of fibers oriented in the aligned (or circumferential) direction. Based on recent models of inter-

layer interactions (Nerurkar, et al., 2011), we further hypothesized that, with increasing time in culture, only multi-layers containing "non-orthogonal" fiber alignment within or between layers would produce inter-layer matrix that conferred an additional mechanical reinforcement effect in the construct.

2. Materials and Methods

2.1. Scaffold Fabrication

Nanofibrous scaffolds composed of poly(ε-caprolactone) (PCL, 80 kDa) were created via electrospinning (5-7). Briefly, PCL was dissolved in equal parts dimethylformamide and tetrahydrofuran (Fisher Chemical) at 40°C (14.3% w/v) and driven through an 18G needle charged to +12kV (Gamma High Voltage Research Inc.) at 2 mL/hr. The needle was situated ~150 mm from the collection mandrel. Separate collection mandrels were designed to collect fibers along the long-axis of a rotating cylinder or the end of a rotating disk (~10 m/s surface velocity) to collect fibers with uniform alignment in a single direction (linearly aligned) or circumferentially aligned, respectively (Fisher, et al., 2013). Mats of ~250µm thickness were formed, and from these, individual scaffolds (5 mm in width x 40 mm in length) were isolated (**Fig. 1A**). From linearly aligned mats, scaffolds were produced such that the long axis was parallel (0°) or perpendicular (90°) to the fiber direction. Additional scaffolds were produced such that the midpoint of the long-axis of the scaffolds was tangent to the radial direction of the fibrous mat, capturing fibers aligned in a circumferential manner (C), as previously described (Fisher, et al., 2013).

2.2. Cell Seeding and Construct Formation

Juvenile bovine MSCs (from two donors of 3-6 months in age) were harvested from the marrow within the femur and tibia and expanded through passage two in Dulbecco's modified Eagle's medium with 10% fetal bovine serum and 1% penicillin/streptomycin/fungizone (Baker, et al., 2008, Baker, et al., 2007). MSCs from the two donors were pooled, mixed thoroughly, and applied evenly to all constructs. Single layer scaffolds (0°, 90°, and C) were sterilized and rehydrated via serial ethanol washes and maintained in sterile phosphate buffered saline (PBS). Prior to seeding, scaffolds were coated with fibronectin (20 µg/ml) in PBS for 12 hours and washed with PBS. MSCs (0.5 million in 100 µl of DMEM) were seeded on each side of each scaffold followed by a one hour incubation at 37°C. Afterward, scaffolds were cultured in a chemically-defined media containing TGF-β3 (10 ng/ml) at 37°C and 5%CO_2 for one week (1ml of media per construct) (Mauck, et al., 2006).

After one week, multi-layer scaffolds, consisting of three scaffold layers, were formed by placing individual layers in apposition as previously described (Nerurkar, et al., 2009). Specifically, multi-layer constructs were placed between porous polypropylene scaffolds, and the assembly was held together using a foil cinch (**Fig. 1B**). Five multi-layer groups were created: 1) 0°/0°/0°, 2) 90°/90°/90°, 3) 0°/90°/0°, 4) 90°/0°/90°, and 5) C/C/C (**Fig. 1C**). Single-layer and multi-layer constructs (n=7 per group) were then cultured in chemically-defined media with TGF-β3 (10 ng/mL) (1 mL and 3 mL of media per construct, respectively) for an additional 2 or 5 weeks (for a total of 3 or 6 weeks of culture). After 2 weeks of culture, polypropylene supports were removed, and constructs

7

were cultured freely. Upon removal of the foil cinch, the layers within the constructs remained adhered to each other for the entirety of the experiment.

2.3. Mechanical Testing

Prior to testing, the cross-sectional area of the samples (n=5/group) was measured using a custom laser-based device, and samples were speckle coated with Verhoeff's stain for strain analysis. Constructs were placed in custom-made grips with a clamp-to-clamp length of ~25 mm (aspect ratio of ~5) in a materials testing machine (model 5848, Instron). Within a saline bath maintained at 37°C, samples were preloaded to 0.5N, preconditioned from 0-3% strain for 15 cycles, and extended to failure at a rate of 0.5%/sec. During the load-to-failure test, images of the sample were acquired at a rate of 2 frames per second.

From the resulting load-elongation curve, stiffness was calculated as the maximum slope over a 1 mm range of elongation in the linear region. To calculate tensile modulus, force was divided by the original cross-sectional area of the specimen. Additionally, Lagrangian strain along the direction of loading (within an area representing the central 50% of the specimen along its length) was computed using image correlation software (Vic2D, Correlated Solutions). From the resulting stress-strain curve, tensile modulus was calculated as the maximum slope of the linear region of the stress-strain over a 5% strain range. As an alternative, the modulus was also calculated between 5% and 10% strain.

To test for interactive effects within multi-layer scaffolds, data acquired from single layer constructs were used to predict the stiffness of multi-layer scaffolds.

Specifically, assuming no interactive effects between the layers, the stiffness of the multi-layer scaffolds could be represented as three single-layer scaffolds acting in parallel. As such, predicted stiffness for the multi-layer scaffolds was calculated as the sum of the stiffness of three single layer scaffolds with similar alignment, using the mean stiffness value for the single layer groups at the appropriate time point. The percent difference between the experimental and predicted stiffness represented the interaction effect, and these values were used for comparisons between groups.

2.4. Histological Assessment

For histological assessment (n=2/group), scaffolds were embedded in optimal cutting temperature compound (Tissue-Tek O.C.T. compound, Sakura Finetek) and sectioned (16µm thickness). Sections were collected perpendicular to the long axis of the scaffolds (cross-sectional), parallel to the long axis (*en face*), or at an angle near parallel to the long axis (angled) (**Fig. 6**). To evaluate cellular colonization, nuclei were visualized with 4', 6-diamidino-2-phenylindole (DAPI) and imaged via fluorescent microscopy (Eclipse 90i, Nikon Instruments). Collagen distribution was assessed by picrosirius red staining and imaging via light microscopy. Additional picrosirius red stained sections were viewed under polarized light microscopy to visualize collagen organization.

2.5. Collagen Content

Following mechanical testing, the central portion of each specimen (20 mm length) was collected. Matrix components were solubilized via papain digestion at 60°C

for 24 hours. Collagen content was quantified using the orthohydroxyproline assay (Stegemann, et al., 1967). An OHP:collagen ratio of 7.14 was used to convert µg of OHP to µg of collagen (Neuman, et al., 1950). Predicted collagen content at 6 weeks of culture was computed for the multi-layer groups based on single-layer data, following a similar approach as used for the stiffness measures.

2.6. Statistical Analysis

Statistical analyses were completed using SPSS (version 22, IBM Corp.). Comparisons were done separately for the single layer groups and multi-layer groups. Normality of each group was confirmed via the Kolmogorov-Smirnoff test. Two-way analysis of variance (ANOVA) was performed with experimental group and culture time as main effects. If necessary, Bonferroni or Games-Howell post-hoc tests were done between individual groups, depending on whether the variances were or were not equal, respectively. For prediction of stiffness and collagen content of multi-layer scaffolds, differences between the experimental and predicted values were compared using a one-way ANOVA and Bonferroni post-hoc tests. Finally, Pearson correlation coefficients were calculated to relate the collagen content of the scaffolds to their stiffness or modulus values. For all analyses, overall significance was maintained at $p<0.05$.

3. Results

3.1. Mechanical Analysis of Single- and Multi-Layered Constructs

Prior to testing, all constructs were robust, and no failure or separation of layers was observed due to handling. In examining the load-elongation and stress-strain curves,

10

the toe region was prominent for all groups except for those only featuring fibers running perpendicular to the direction of loading (90° single layer and 90°/90°/90° multilayer scaffolds). For all other groups, the toe region was similar and continued until ~5-6% strain. All groups featured a linear region before yield and eventual failure.

For single layer constructs (**Fig. 2**), the two-way ANOVA of stiffness revealed significant effects due to group and time in culture ($p<0.05$) as well as a significant interaction term ($p<0.05$). Post-hoc tests showed that scaffolds aligned in the direction of testing (0°) had stiffness values an order of magnitude higher than perpendicularly aligned scaffolds (90°) at both time points ($p<0.05$). By 6 weeks, these values were 120% higher than those of the circumferentially aligned scaffolds (C) ($p<0.05$). At both time points, the stiffness of circumferentially aligned scaffolds also reached values 7-fold higher than those of the 90° group ($p<0.05$). Only the 0° group significantly increased from 3 to 6 weeks ($p<0.05$).

For multi-layer scaffolds (**Fig. 2**), a significant effect was found for both experimental group and time in culture ($p<0.05$), with no significant interaction term ($p>0.05$). As such, post-hoc comparisons between scaffold groups were not separated with respect to time. As expected, the stiffness of the 0°/0°/0° scaffolds were higher than all other groups ($p<0.05$), while the 90°/90°/90° scaffolds were several fold lower than all other groups ($p<0.05$). Interestingly, no significant differences could be determined between the 0°/90°/0° and C/C/C groups ($p>0.05$), and these groups had stiffness values 40-75% higher relative to the 90°/0°/90° scaffolds ($p<0.05$).

To assess the quality of the constructs and account for differences in size between groups, the tensile modulus of the constructs was also computed (**Fig. 3**). The trends

11

between groups were similar between the two calculations of modulus (maximum slope and slope from 5-10% strain). As such, only the data from the former method are presented. Analysis of single layer scaffolds revealed similar findings as those for stiffness. Namely, the 0° groups were 28-to 45-fold and 2-3 fold higher than the 90° and C groups, respectively (p<0.05). Moreover, the C groups were 11- to 18-fold higher than 90° groups (p<0.05).

For the modulus of multi-layer scaffolds, a significant effect was found for culture time (p<0.05), and there was a significant interaction between culture time and group (p<0.05). Only the 90°/90°/90° scaffolds changed with culture time (85% increase from 3 to 6 weeks, p<0.05), although their absolute values were the lowest for any experimental group at either time point. At 3 weeks, all experimental groups were different from one another (p<0.05), with the 90°/0°/90° and C/C/C groups being the lone exception (p>0.05). At 6 weeks, only the 0°/0°/0° and 90°/90°/90° were significantly different (11-fold difference, p<0.05), while all other experimental groups had similar values (p>0.05).

3.2. Histological and Biochemical Analysis of Single- and Multi-Layered Constructs

At 3 and 6 weeks of culture, collagenous matrix accumulated both within scaffold layers as well as at their peripheries for both single layer and multi-layer constructs (6 week data shown in **Fig. 4 & 5**, respectively). Generally, the intensity of staining increased from 3 to 6 weeks of culture for all scaffold groups, independent of layering and organization. For multi-layer constructs, deposition of matrix between layers enabled removal of the supports a two weeks without dehiscence. Additionally, MSCs infiltrated into the majority of the scaffold thickness, with only the central region devoid of cells

12

(**Figs. 4 & 5**). As with collagen deposition, cell colonization was independent of alignment (0°, 90°, or C) as well as whether the scaffold layers were cultured as single layers or multi-layers.

Polarized light imaging of the multi-layer constructs showed organization of newly formed collagen. By sectioning the constructs parallel to layers (*en face*), collagen organization within a layer could be visualized (data not shown). Alignment of this newly formed collagenous matrix followed the direction of the scaffold fibers for all multi-layer constructs, independent of the type of alignment within the layer (0°, 90°, or C). Additional multi-layer scaffolds were sectioned at a steeper angle (**Fig. 6**), allowing the visualization of alignment within multiple layers in the same image. Most interestingly, images that captured the interface between two layers of different alignment (such as those in the 0°/90°/0° and 90°/0°/90° multi-layers) revealed that the matrix at or near these interfaces maintained the alignment of the individual scaffold layers.

Collagen content for all constructs was also quantified (**Fig. 7**). For single layer groups, the two-way ANOVA indicated no statistically significant effects between groups or with culture time (p>0.05). Similar levels of collagen were also found between the multi-layer groups (p>0.05), with a 32-389% increase from 3 to 6 weeks of culture within individual multi-layer groups (p<0.05). Considering all samples, collagen content was mildly correlated to stiffness (R^2=0.39, p<0.05), but no correlation was established between collagen content and modulus (R^2=0.05, p>0.05). These correlation coefficients were similar if only individual time points were considered or if single layer and multi-layer groups were analyzed separately (data not shown).

3.3. Prediction of Multi-Layered Construct Performance based on Single Layer Constructs

To determine the impact and interactions within multi-layer constructs, collagen content and stiffness data for single layer constructs was used to predict the expected data for multi-layer groups at 6 weeks (**Fig. 8**). For collagen content, data showed a general positive effect for multi-layer construction relative to single layer construction, with up to 100% more collagen content than expected for some groups (though there was little effect in the C/C/C group) (**Fig. 8A**). No statistically significant differences were found between multi-layer groups (p>0.05). Conversely, for stiffness, only the C/C/C group had a positive interactive effect (56%, **Fig. 8B**). Multi-layer groups with two or more 0° layers (0°/0°/0° and 0°/90°/0°) had the greatest negative interaction (-82% and -66%, respectively), while multi-layer groups with two or more 90° layers (90°/90°/90° and 90°/0°/90°) had mean values near zero (-1% and -10%, respectively), indicating little interaction between layers. Statistical analysis revealed that the C/C/C group had an interaction that was significantly more positive than the 0°/0°/0° and 0°/90°/0° groups (p<0.05).

4. Discussion

In this work, we evaluated the impact of varying fiber alignment within single layer and multi-layer MSC-seeded electrospun nanofibrous scaffolds designed for meniscus tissue engineering. We compared single-layer scaffolds featuring fiber alignment in a single direction (parallel (0°) or perpendicular (90°)) to scaffolds in which the fibers were preferentially aligned in a circumferential pattern along the length of the

14

scaffold (C). In addition, we assessed the impact of varying the combination of layers with alignment parallel or perpendicular to the testing direction in multi-layer constructs, mimicking the orthogonal arrangement of circumferential and radial tie fibers in native tissue. In support of our first hypothesis, different fiber orientations within scaffold layers comprising the multi-layered constructs did in fact yield different mechanical outcomes, with higher tensile properties in constructs containing more fibers aligned with the direction of testing. Furthermore, and consistent with our second hypothesis, only multi-layers with "non-orthogonal" alignment within layers (C/C/C) showed evidence for a mechanical reinforcement effect.

MSC-seeded single layer constructs served as the building blocks for the multi-layer constructs. As expected, single layer constructs featuring circumferentially aligned fibers had mechanical characteristics that were lower than, but closest to, the 0° configuration, while the values for the 90° configuration were several fold lower. These data are consistent with our previous work comparing acellular 0° and C scaffolds, where we determined that the tensile modulus of acellular C scaffolds was 50-75% lower than the 0° scaffolds (Fisher, et al., 2013). We further showed in that study that these mechanical differences were likely due to increased fiber rotation in the C scaffolds resulting in greater shear strain, particularly in regions where fibers were oriented at greatest angles from the direction of loading.

Building from these single layer constructs, we next assembled, cultured, and evaluated multi-layered constructs consisting of MSC-seeded scaffold layers with varying alignment. 0°/0°/0° constructs had the highest stiffness and modulus values while 90°/90°/90° constructs had the lowest values, with the 0°/90°/0° and 90°/0°/90°

constructs falling in between these extremes, confirming our first hypothesis. C/C/C scaffolds produced values closest to the 0°/90°/0° group. Together with the data for the single layer constructs, these data indicate that the structural hierarchies 'engineered in' to multi-lamellar composites dictate the overall functional properties of cell-seeded composites during maturation.

An additional hypothesis evaluated in this work was that only the C/C/C multi-layered constructs, which featured "non-orthogonal" alignment between layers would exhibit a mechanical reinforcement effect. This hypothesis was based on previous experimental and theoretical work in MSC-seeded bi-layer constructs. Nerurkar et al. tested two configurations, layers with parallel alignment (+30°/+30°) or layers offset in opposite directions (-30°/+30°) relative to the direction of loading (Nerurkar, et al., 2009). Interestingly, the -30°/+30° constructs had a higher modulus relative to the +30°/+30° constructs due to the resistance of the inter-layer matrix to shear, resulting in a reinforcement effect. These findings were confirmed through biaxial testing as well as through additional experimental configurations and computational modeling (Driscoll, et al., 2011, Nerurkar, et al., 2011). Modeling predicted that minimal interaction stresses would occur when the fiber angle between layers was 0° or 90° (Nerurkar, et al., 2011). This model also predicted that coherent fiber rotation within layers upon extension of the construct was necessary for the generation of interaction stresses between layers.

To test these mechanisms in three-layer constructs, we extrapolated the data for the single layer constructs to predict the multi-layer scenario. In support of our second hypothesis, only the C/C/C constructs had a positive reinforcement effect (i.e. an experimental stiffness that exceeded the predicted stiffness). Based on the previous

16

computational work (Nerurkar, et al., 2011), layers with similar (e.g. 0°/0°/0°) or perpendicular (0°/90°/0°) aligned layers would be expected to produce little rotation between layers with tensile loading, and thus, we would not have expected to see a reinforcement effect. In fact, for certain configurations, such as the 0°/0°/0° scaffolds, the large amount of matrix produced on the surface or outside of the scaffolds may have contributed to the reduced stiffness of the constructs relative to predicted values. For the C/C/C scaffolds, although the scaffold layers were aligned in the same direction, fiber alignment within each layer continuously changed, and these fibers rotate upon elongation, producing high shear strains (Fisher, et al., 2013). Collagenous reinforcement between nanofibers may have therefore helped to resist rotation of the fibers and matrix during tensile deformation, producing the observed positive reinforcement effect. It remains to be determined if the addition of a layer with opposing alignment placed between these layers could further enhance this reinforcement effect.

To further understand the mechanisms for the difference in mechanics between the single layer and multi-layer scaffolds, we examined the formation of collagen and its alignment. All constructs showed similar degrees of cell infiltration and collagen production independent of the alignment of the scaffold. While we did not directly measure porosity or pore size, linearly aligned and circumferentially aligned fibers possess similar features on the nanoscale (Fisher, et al., 2013), so it was not surprising to find similar levels of cell infiltration. The similar collagen production is consistent with previous work by Baker et al., where cells on highly aligned and randomly aligned scaffolds produced similar amounts of collagen (Baker, et al., 2007), suggesting that fiber alignment does not influence production rates. Of note, predicted collagen content in

17

multi-layer constructs was generally higher than predictions from single-layer constructs. This observation may be related to an increased retention of newly produced collagen between layers. While overall levels were not different, deposited collagen did align along the nanofiber direction for all constructs, as evidenced by polarized light microscopy. Again, this is consistent with previous work showing that cells align along fibers, via contact guidance, which in turn directs the formation of new collagen in a similar direction (Baker, et al., 2007, Baker, et al., 2010, Wang, et al., 2000). Interestingly, the amount of collagen produced was mildly correlated to the stiffness of the constructs as expected, but not their modulus. Thus, the differences in mechanical properties (i.e. modulus) in the constructs, which are decoupled from specimen size, were the result of differences in scaffold alignment, and later, new collagenous matrix alignment, but not due to the total amount of collagen.

While this study sheds new light on how structural hierarchies beget complex mechanical function in multi-layered nanofibrous assemblies, there exist several limitations. First, we utilized only three layers in our multi-layer scaffolds, and so constructs were still considerably thinner than the native meniscus (~1 mm vs. ~10 mm). Since our intention was to capture and quantify changes with different multi-layer configurations, using only three layers allowed us to do so, without introducing additional complicating factors. In the future, it will be critical to test larger, anatomically sized scaffolds to evaluate additional factors, such as nutrient limitations, that could compromise matrix accumulation (Farrell, et al., 2014). Additionally, this study was not powered to provide quantitative data from the histological images, so we did not quantify matrix alignment or fiber/bundle size, although we note that both the fibers within the

scaffold and those within the formed collagenous matrix remain quite small. It may well be that longer culture durations and or biophysical stimulation will be required to foster fiber network aggregation and maturation to match native tissue levels, as has been shown in collagen gel-based engineered meniscus constructs (Puetzer, et al., 2013). Finally, we believe the increased collagen content in the multi-layer scaffolds could be an effect of diffusion, where the thicker composition traps or retains more collagen in the constructs. However, the amount of collagen in the culture media was not measured, so it is unclear if the cells in the multi-layer scaffolds made more collagen than the cells in the single layers or if more was just localized within the construct.

In the future, it will be essential to explore the addition of a "radial layer" in between the circumferentially aligned scaffold layers to further mimic the structure of the meniscus.   Moreover, longer time points could be employed to increase overall mechanical properties of MSC-laden constructs, as previous studies have noted large changes in mechanics from 6 to 12 weeks, as the newly produced matrix coalesces to result in a construct with increased material quality, not just size (Baker, et al., 2012). Sacrificial fiber fractions could also be employed to increase scaffold porosity in order to enhance intra-lamellar cellular infiltration and matrix deposition, while mechanical stimulation could be used to expedite matrix deposition (Baker, et al., 2011, Baker, et al., 2012). Future work will also more fully characterize these multi-lamellar constructs in more complex loading configurations, such as biaxial loading, or the use of knee simulators or robotic systems (Driscoll, et al., 2013, Fisher, et al., 2011, Maher, et al., 2010).

A successful tissue engineered meniscus should match the complex geometry and unique mechanical and structural features of the native tissue at both the microscopic and macroscopic scale. The current work built from previous work using single layers of nanofibrous fibers to produce a 3D multi-layered engineered meniscus construct that captured the microscopic and macroscopic structure, organization, and function of the native meniscus, inclusive of orthogonal layers (representing circumferential and radial tie fibers). As these multi-layer constructs become increasingly complex and more faithfully reproduce native tissue structural hierarchies, they may not only serve as functional substitutes for implantation for meniscus repair, but may also provide test beds in which to probe and understand the mechanical principles that enable meniscus function in a complex loading environment.

Conflict of interest statement

The authors have no disclosures or conflicts of interest to report.

References

Ahmed, A. M., Burke, D. L., 1983. In-vitro measurement of static pressure distribution in synovial joints--part i: Tibial surface of the knee. J Biomech Eng 105(3), 216-225.

Andrews, S. H., Rattner, J. B., Abusara, Z., Adesida, A., Shrive, N. G., Ronsky, J. L., 2014. Tie-fibre structure and organization in the knee menisci. J Anat 224(5), 531-537.

Aufderheide, A. C., Athanasiou, K. A., 2007. Assessment of a bovine co-culture, scaffold-free method for growing meniscus-shaped constructs. Tissue Eng 13(9), 2195-2205.

Baker, B. M., Gee, A. O., Metter, R. B., Nathan, A. S., Marklein, R. A., Burdick, J. A., Mauck, R. L., 2008. The potential to improve cell infiltration in composite fiber-aligned electrospun scaffolds by the selective removal of sacrificial fibers. Biomaterials 29(15), 2348-2358.

Baker, B. M., Mauck, R. L., 2007. The effect of nanofiber alignment on the maturation of engineered meniscus constructs. Biomaterials 28(11), 1967-1977.

Baker, B. M., Nathan, A. S., Gee, A. O., Mauck, R. L., 2010. The influence of an aligned nanofibrous topography on human mesenchymal stem cell fibrochondrogenesis. Biomaterials 31(24), 6190-6200.

Baker, B. M., Shah, R. P., Huang, A. H., Mauck, R. L., 2011. Dynamic tensile loading improves the functional properties of mesenchymal stem cell-laden nanofiber-based fibrocartilage. Tissue Eng Part A 17(9-10), 1445-1455.

Baker, B. M., Shah, R. P., Silverstein, A. M., Esterhai, J. L., Burdick, J. A., Mauck, R. L., 2012. Sacrificial nanofibrous composites provide instruction without impediment and enable functional tissue formation. Proc Natl Acad Sci U S A 109(35), 14176-14181.

Balint, E., Gatt, C. J., Jr., Dunn, M. G., 2012. Design and mechanical evaluation of a novel fiber-reinforced scaffold for meniscus replacement. J Biomed Mater Res A 100(1), 195-202.

Ballyns, J. J., Bonassar, L. J., 2011. Dynamic compressive loading of image-guided tissue engineered meniscal constructs. J Biomech 44(3), 509-516.

Bedi, A., Kelly, N. H., Baad, M., Fox, A. J., Brophy, R. H., Warren, R. F., Maher, S. A., 2010. Dynamic contact mechanics of the medial meniscus as a function of radial tear, repair, and partial meniscectomy. J Bone Joint Surg Am 92(6), 1398-1408.

Bursac, P., York, A., Kuznia, P., Brown, L. M., Arnoczky, S. P., 2009. Influence of donor age on the biomechanical and biochemical properties of human meniscal allografts. Am J Sports Med 37(5), 884-889.

Cook, J. L., Fox, D. B., Malaviya, P., Tomlinson, J. L., Kuroki, K., Cook, C. R., Kladakis, S., 2006. Long-term outcome for large meniscal defects treated with small intestinal submucosa in a dog model. Am J Sports Med 34(1), 32-42.

Driscoll, T. P., Nakasone, R. H., Szczesny, S. E., Elliott, D. M., Mauck, R. L., 2013. Biaxial mechanics and inter-lamellar shearing of stem-cell seeded electrospun angle-ply laminates for annulus fibrosus tissue engineering. J Orthop Res (in press).

Driscoll, T. P., Nerurkar, N. L., Jacobs, N. T., Elliott, D. M., Mauck, R. L., 2011. Fiber angle and aspect ratio influence the shear mechanics of oriented electrospun nanofibrous scaffolds. J Mech Behav Biomed Mater 4(8), 1627-1636.

Farrell, M. J., Shin, J. I., Smith, L. J., Mauck, R. L., 2014. Functional consequences of glucose and oxygen deprivation on engineered mesenchymal stem cell-based cartilage constructs. Osteoarthritis Cartilage.

Fisher, M. B., Henning, E. A., Soegaard, N., Esterhai, J. L., Mauck, R. L., 2013. Organized nanofibrous scaffolds that mimic the macroscopic and microscopic architecture of the knee meniscus. Acta Biomater 9(1), 4496-4504.

Fisher, M. B., Jung, H. J., McMahon, P. J., Woo, S. L., 2011. Suture augmentation following ACL injury to restore the function of the ACL, MCL, and medial meniscus in the goat stifle joint. J Biomech 44(8), 1530-1535.

Fithian, D. C., Kelly, M. A., Mow, V. C., 1990. Material properties and structure-function relationships in the menisci. Clin Orthop Relat Res (252), 19-31.

Garrett, W. E., Jr., Swiontkowski, M. F., Weinstein, J. N., Callaghan, J., Rosier, R. N., Berry, D. J., Harrast, J., Derosa, G. P., 2006. American board of orthopaedic surgery practice of the orthopaedic surgeon: Part-ii, certification examination case mix. J Bone Joint Surg Am 88(3), 660-667.

Greis, P. E., Bardana, D. D., Holmstrom, M. C., Burks, R. T., 2002. Meniscal injury: I. Basic science and evaluation. J Am Acad Orthop Surg 10(3), 168-176.

Greis, P. E., Holmstrom, M. C., Bardana, D. D., Burks, R. T., 2002. Meniscal injury: Ii. Management. J Am Acad Orthop Surg 10(3), 177-187.

Heijkants, R. G., van Calck, R. V., De Groot, J. H., Pennings, A. J., Schouten, A. J., van Tienen, T. G., Ramrattan, N., Buma, P., Veth, R. P., 2004. Design, synthesis and properties of a degradable polyurethane scaffold for meniscus regeneration. J Mater Sci Mater Med 15(4), 423-427.

Kelly, B. T., Robertson, W., Potter, H. G., Deng, X. H., Turner, A. S., Lyman, S., Warren, R. F., Rodeo, S. A., 2007. Hydrogel meniscal replacement in the sheep knee: Preliminary evaluation of chondroprotective effects. Am J Sports Med 35(1), 43-52.

Kurosawa, H., Fukubayashi, T., Nakajima, H., 1980. Load-bearing mode of the knee joint: Physical behavior of the knee joint with or without menisci. Clin Orthop Relat Res (149), 283-290.

Lubowitz, J. H., Poehling, G. G., 2011. Save the meniscus. Arthroscopy 27(3), 301-302.

Maher, S. A., Rodeo, S. A., Doty, S. B., Brophy, R., Potter, H., Foo, L. F., Rosenblatt, L., Deng, X. H., Turner, A. S., Wright, T. M., Warren, R. F., 2010. Evaluation of a porous polyurethane scaffold in a partial meniscal defect ovine model. Arthroscopy 26(11), 1510-1519.

Makris, E. A., Hadidi, P., Athanasiou, K. A., 2011. The knee meniscus: Structure-function, pathophysiology, current repair techniques, and prospects for regeneration. Biomaterials 32(30), 7411-7431.

Mandal, B. B., Park, S. H., Gil, E. S., Kaplan, D. L., 2012. Multilayered silk scaffolds for meniscus tissue engineering. Biomaterials 32(2), 639-651.

Mauck, R. L., Yuan, X., Tuan, R. S., 2006. Chondrogenic differentiation and functional maturation of bovine mesenchymal stem cells in long-term agarose culture. Osteoarthritis Cartilage 14(2), 179-189.

Nerurkar, N. L., Baker, B. M., Sen, S., Wible, E. E., Elliott, D. M., Mauck, R. L., 2009. Nanofibrous biologic laminates replicate the form and function of the annulus fibrosus. Nat Mater 8(12), 986-992.

Nerurkar, N. L., Mauck, R. L., Elliott, D. M., 2011. Modeling interlamellar interactions in angle-ply biologic laminates for annulus fibrosus tissue engineering. Biomech Model Mechanobiol 10(6), 973-984.

Neuman, R. E., Logan, M. A., 1950. The determination of hydroxyproline. J Biol Chem 184(1), 299-306.

Petersen, W., Tillmann, B., 1998. Collagenous fibril texture of the human knee joint menisci. Anat Embryol (Berl) 197(4), 317-324.

Petty, C. A., Lubowitz, J. H., 2011. Does arthroscopic partial meniscectomy result in knee osteoarthritis? A systematic review with a minimum of 8 years' follow-up. Arthroscopy 27(3), 419-424.

Proctor, C. S., Schmidt, M. B., Whipple, R. R., Kelly, M. A., Mow, V. C., 1989. Material properties of the normal medial bovine meniscus. J Orthop Res 7(6), 771-782.

Puetzer, J. L., Bonassar, L. J., 2013. High density type i collagen gels for tissue engineering of whole menisci. Acta Biomater 9(8), 7787-7795.

Sihvonen, R., Paavola, M., Malmivaara, A., Itala, A., Joukainen, A., Nurmi, H., Kalske, J., Jarvinen, T. L., Finnish Degenerative Meniscal Lesion Study, G., 2013. Arthroscopic partial meniscectomy versus sham surgery for a degenerative meniscal tear. N Engl J Med 369(26), 2515-2524.

Skaggs, D. L., Warden, W. H., Mow, V. C., 1994. Radial tie fibers influence the tensile properties of the bovine medial meniscus. J Orthop Res 12(2), 176-185.

Stegemann, H., Stalder, K., 1967. Determination of hydroxyproline. Clin Chim Acta 18(2), 267-273.

Stone, K. R., Rodkey, W. G., Webber, R., McKinney, L., Steadman, J. R., 1992. Meniscal regeneration with copolymeric collagen scaffolds. In vitro and in vivo studies evaluated clinically, histologically, and biochemically. Am J Sports Med 20(2), 104-111.

Veth, R. P., Jansen, H. W., Leenslag, J. W., Pennings, A. J., Hartel, R. M., Nielsen, H. K., 1986. Experimental meniscal lesions reconstructed with a carbon fiber-polyurethane-poly(l-lactide) graft. Clin Orthop Relat Res (202), 286-293.

Wang, J. H., Grood, E. S., 2000. The strain magnitude and contact guidance determine orientation response of fibroblasts to cyclic substrate strains. Connect Tissue Res 41(1), 29-36.

Zielinska, B., Donahue, T. L., 2006. 3d finite element model of meniscectomy: Changes in joint contact behavior. J Biomech Eng 128(1), 115-123.

8. Figure Legends

Figure 1. Schematic of experimental groups. A) Individual scaffolds of varying fiber alignment (fibers parallel to scaffold long axis (0°), fibers perpendicular to scaffold long axis (90°), and comprised of circumferential (C) fibers) were seeded with juvenile bovine mesenchymal stem cells (MSCs) and cultured as single layer or multi-layer constructs. B) Assembly method for the production and culture of multi-layer constructs. C) Illustration of multi-layer groups with different fiber alignment in each layer.

26

Figure 2. Tensile stiffness of single layer and multi-layer constructs after 3 and 6 weeks of culture (*p<0.05 vs. 3w time point, +p<0.05 between experimental groups at both time points, #p<0.05 between experimental groups at 3 weeks, $p<0.05 between experimental groups at 6 weeks).

Figure 3. Tensile modulus of single layer and multi-layer constructs after 3 and 6 weeks of culture (*p<0.05 vs. 3w time point, +p<0.05 between experimental groups at both time points, #p<0.05 between experimental groups at 3 weeks, $p<0.05 between experimental groups at 6 weeks).

Figure 4. Histological analysis of collagen deposition (picrosirius red staining, top row) and cell infiltration (DAPI staining, bottom row) in single layer constructs after 6 weeks of culture (scale bars = 200 μm).

Figure 5. Histological analysis of collagen deposition (picrosirius red staining, top row) and cell infiltration (DAPI staining, bottom row) in multi-layer constructs after 6 weeks of culture (scale bars = 200 μm).

Figure 6. Collagen alignment within multi-layer constructs assessed by polarized light microscopy. Angled sections show collagen fiber alignment within and between layers (arrows indicate scaffold layer alignment, scale bars = 100 μm).

Figure 7. Collagen content of single-and multi-layer constructs after 3 and 6 weeks of culture (*p<0.05 vs. 3 week time point).

Figure 8. Difference between expected and predicted stiffness and collagen content of multi-layer constructs at 6 weeks of culture based on data from single-layer constructs (#p<0.05 between groups). Positive values indicate a positive interaction effect due to multi-layer culture, while negative values indicate a negative interaction effect.
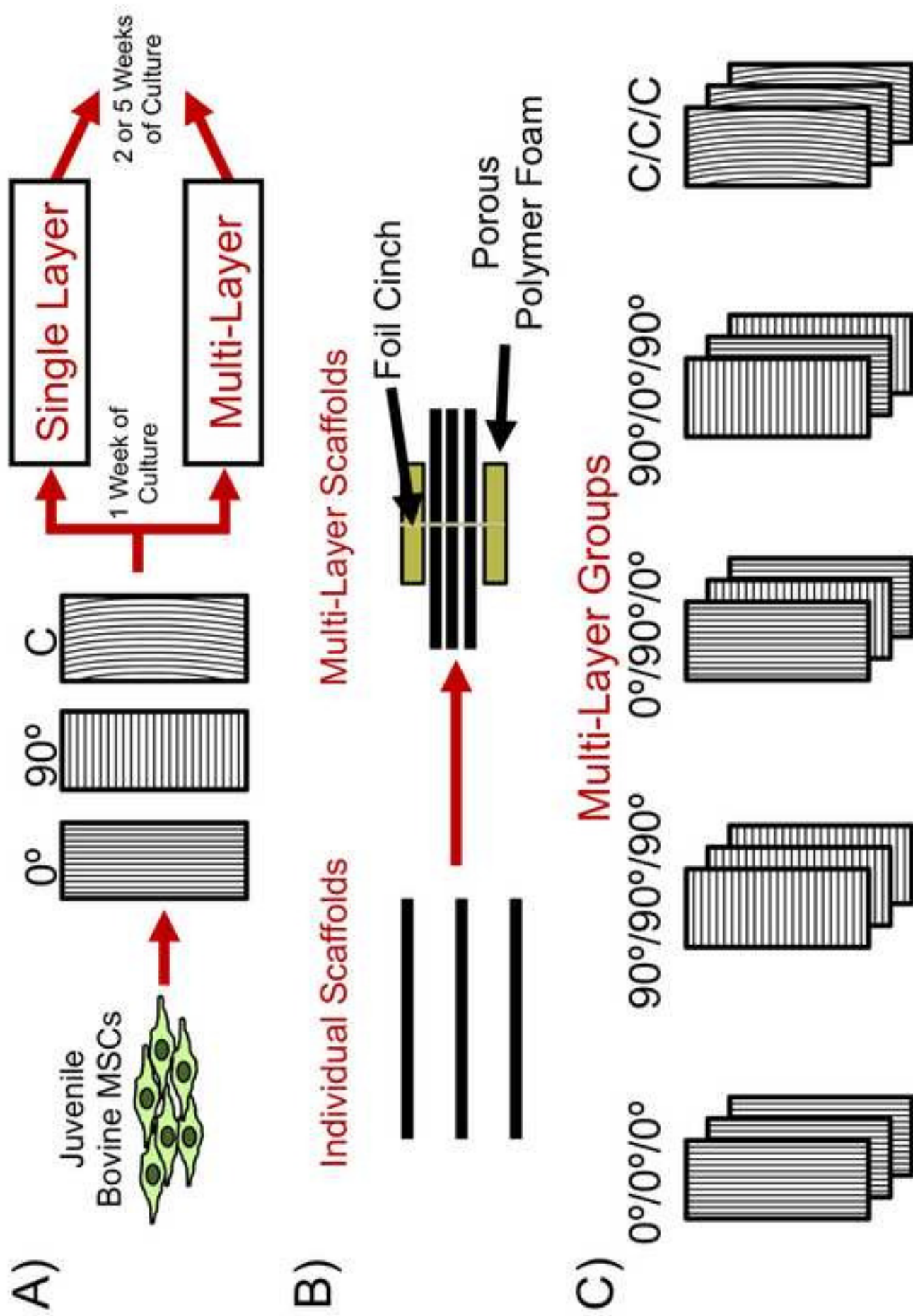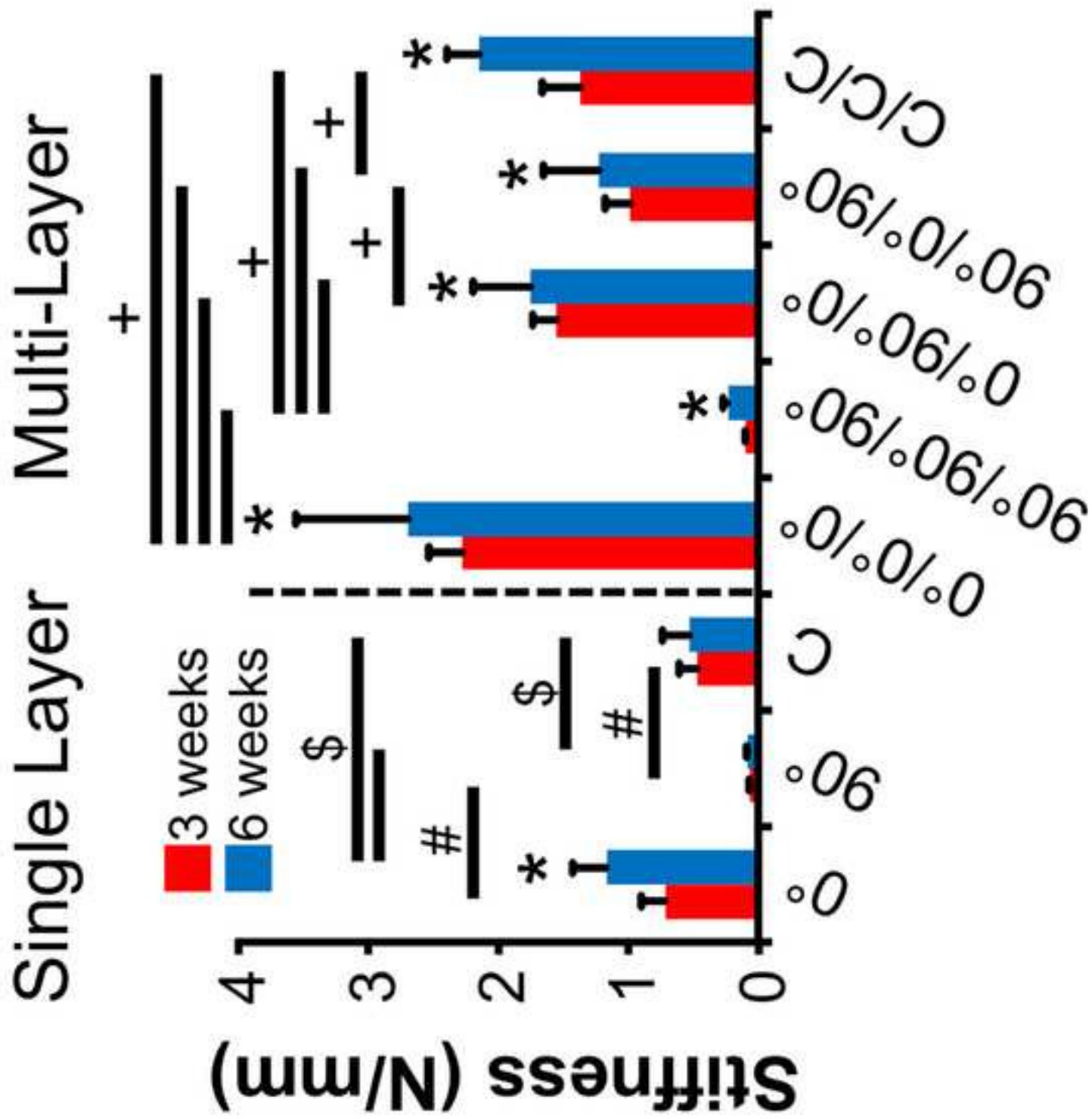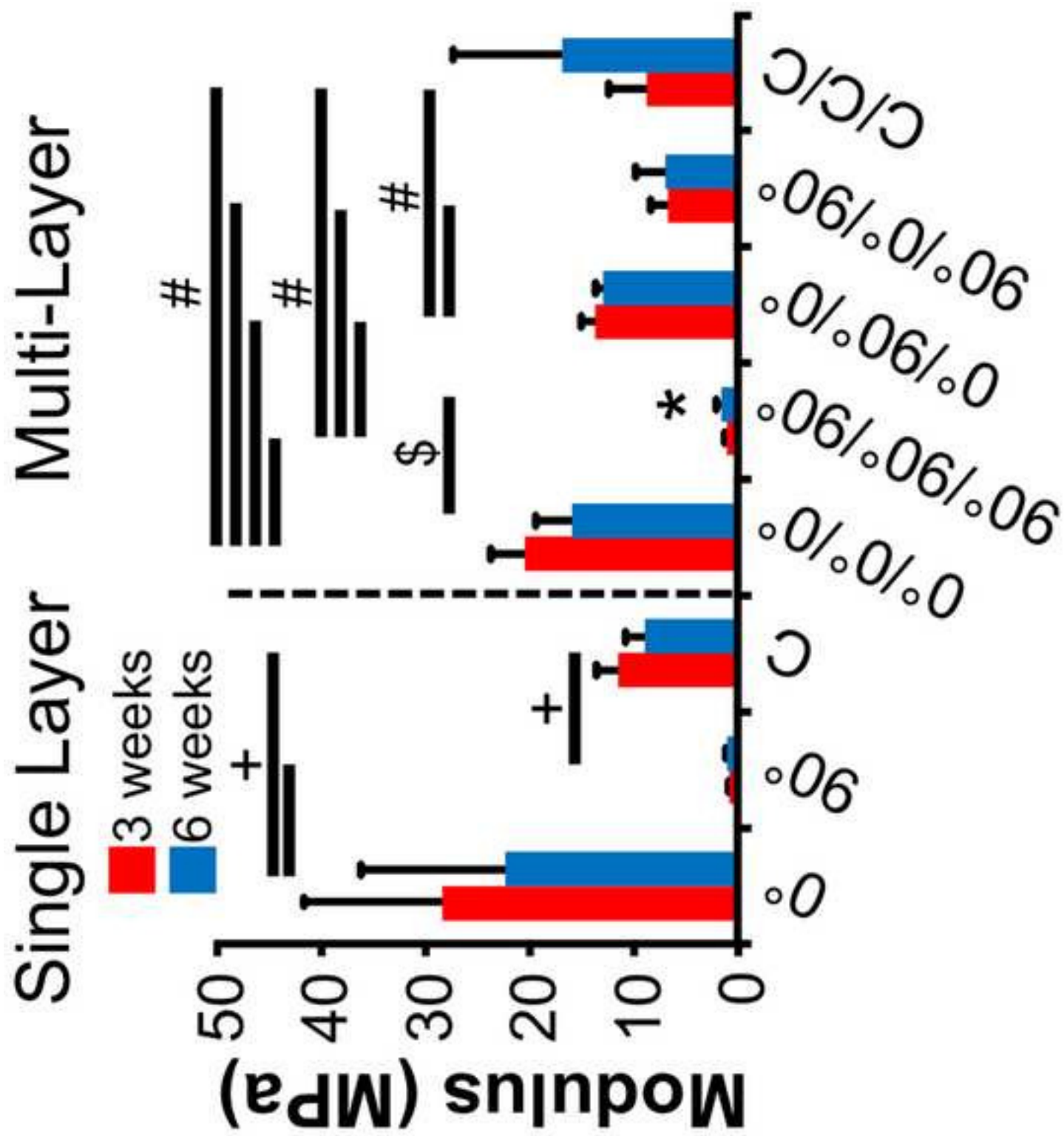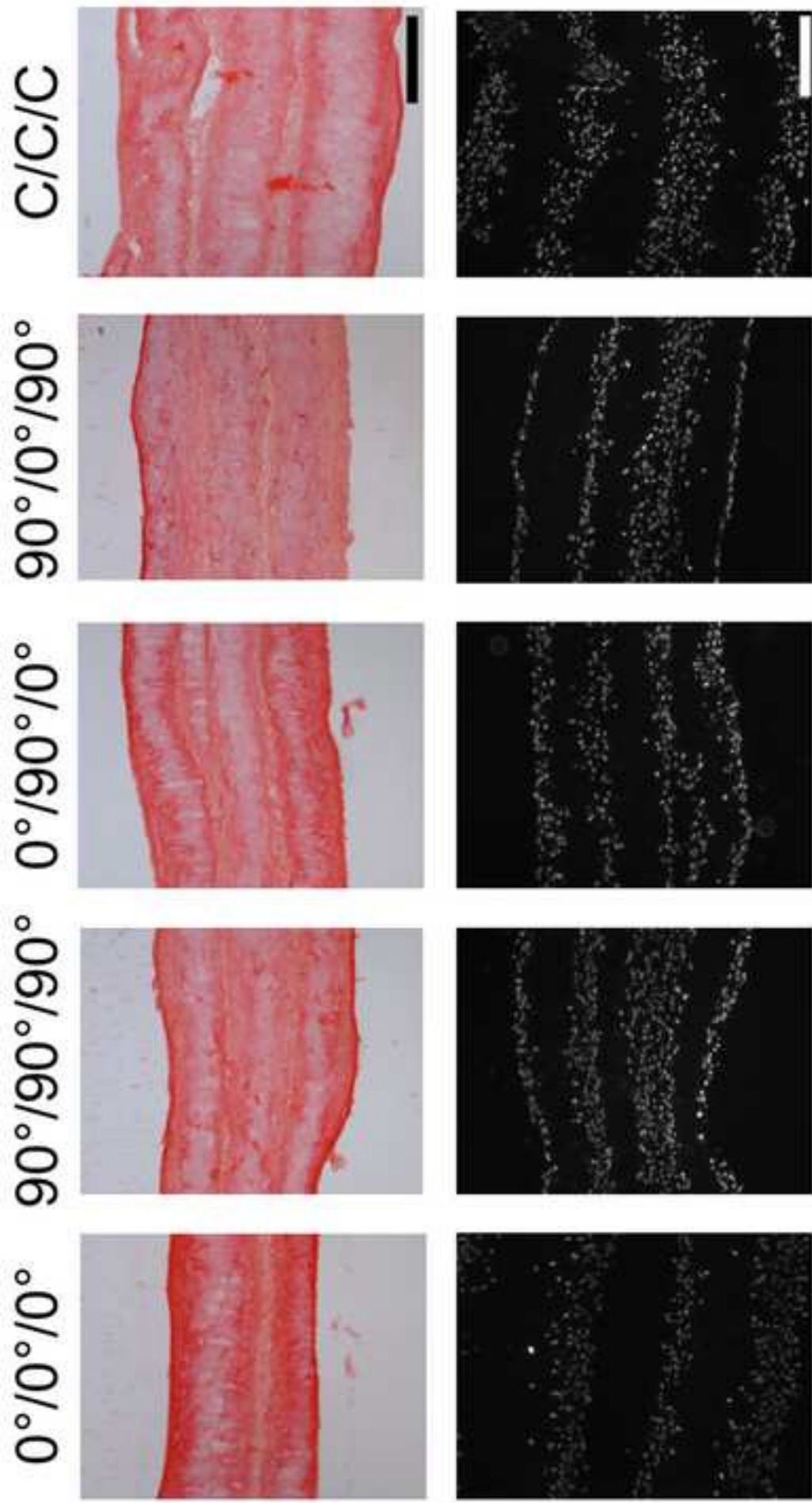
Figure 1

Figure 2

Figure 3
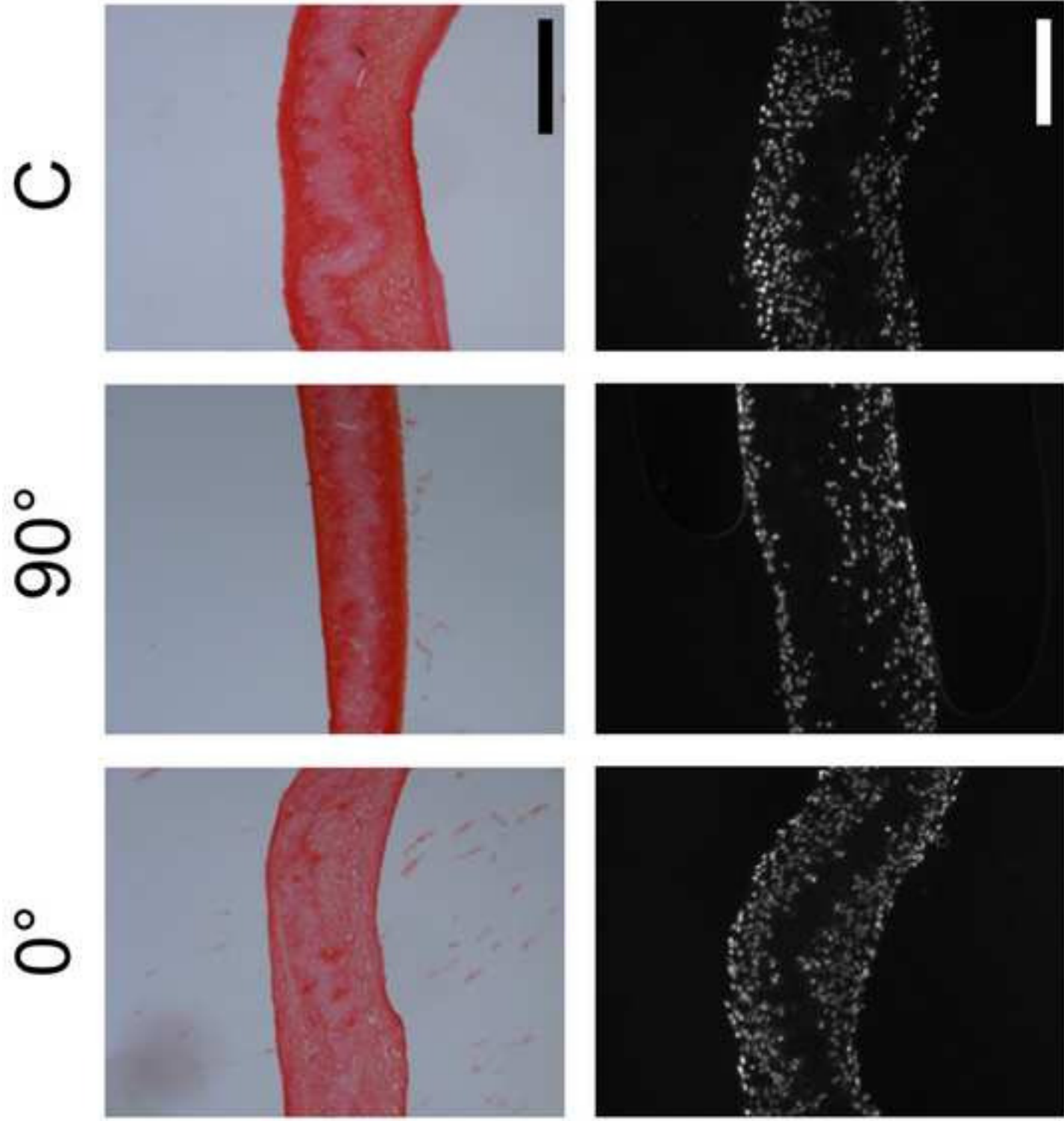
Figure 4

Figure 5

Figure 6

Figure 7

Figure 8